Pantheon+ and Redshift Observational Analysis
of the
UMH Redshift Formulation

Andrew Dodge
Auburn, Washington, USA

Version 1.0.4 - August 2025

Abstract

We present a data-driven observational analysis of the Ultronic Medium Hypothesis (UMH) framework redshift formulation and luminosity relation against Type Ia supernovae in the Pantheon+ sample. Two independent pipelines were applied: (1) a low-z calibration of the UMH redshift relation for $z \leq 0.10$, and (2) a full Pantheon+ Hubble-diagram comparison using the complete STAT+SYS covariance (including statistical and systematic uncertainties). The UMH calibration yields $\alpha = (2.48 \pm 0.08) \times 10^{-4}\,\mathrm{Mpc}^{-1}$, corresponding to $H_0 = 74.4 \pm 2.3\,\mathrm{km\,s^{-1}\,Mpc^{-1}}$.

The UMH formulation contains a single cosmological redshift-scale parameter, α, which is fixed by the low-z calibration, while the coefficients β_1 and β_2 enter only through the broadband transmission function and are held fixed after calibration. Under an explicitly conditional final-fit convention, in which k counts only parameters varied in the final Hubble-diagram likelihood, the UMH fit has $k = 1$, corresponding to the profiled intercept M_0. The flat ΛCDM reference has $k = 2$, corresponding to M_0 and the fitted matter-density parameter Ω_m. Under this convention, the Pantheon+ comparison gives $\Delta\mathrm{AIC} = -2.2$ and $\Delta\mathrm{BIC} = -7.6$.

As an independent validation, applying the same UMH final-fit and transmission-recovery procedure to the DES-SN5YR/ Dovekie Hubble diagram, with α fixed to the Pantheon+/Cepheid calibration, recovers consistent transmission coefficients, $\beta_1 \simeq 0.435$ and $\beta_2 \simeq -0.275$. With these coefficients fixed and only M_0 profiled, the DES-SN5YR UMH fit is statistically indistinguishable from the flat ΛCDM reference fit.

Overall, the UMH formulation reproduces the Pantheon+ distance–redshift relation and the associated $(1+z)$ time-dilation scaling, while the DES-SN5YR recovery test supports interpreting β_1 and β_2 as stable transmission-calibration coefficients rather than Pantheon+-specific fit absorbers. These SN Ia observables alone do not uniquely determine the underlying physical mechanism responsible for cosmological redshift.

1 Introduction

This work presents the observational consequences of the UMH redshift formulation using the Pantheon+ Type Ia supernova dataset. The analysis focuses on the luminosity distance–redshift relation and associated time–dilation behavior, which are directly probed by SN Ia observations. The broader UMH framework, including derivations of its dynamical structure and applications to the cosmic microwave background (CMB), baryon acoustic oscillations (BAO), and gravitational-wave phenomena, is described in [1]. Since SN Ia observations probe only the luminosity distance–redshift relation and associated time dilation, they do not by themselves uniquely determine the underlying physical mechanism responsible for redshift.

1.1 Background

The ***Ultronic Medium Hypothesis (UMH)***[1] is a proposed framework in which spacetime is modeled as a mechanically real, Lorentz-invariant wave medium in which particles, fields, curvature, General Relativity (GR), and Quantum Field Theory (QFT) arise as coherent oscillations of a continuous tensioned substrate. The speed of light corresponds to the medium's intrinsic wave speed, $c = \sqrt{\frac{T_u}{\rho_u}}$, and relativistic invariance emerges without a preferred frame.

The UMH formulation is applied here specifically to its cosmological prediction: in this formulation, redshift and time dilation arise from cumulative energy transfer through the ultronic medium rather than metric expansion. The standard ΛCDM framework models cosmological distance–redshift data through an expansion history containing matter, radiation, curvature assumptions, and a dark-energy component. In contrast, the UMH formulation provides a distinct description of these same SN Ia observables grounded in wave-based propagation dynamics. This paper tests that SN Ia prediction using Pantheon+ Type Ia supernova data.

2 Methods

2.1 Datasets

This study follows the standard SN Ia cosmological analysis pipeline, including use of the full Pantheon+ STAT+SYS covariance matrix, nuisance-parameter profiling, and goodness-of-fit evaluation via χ^2, AIC, and BIC statistics, enabling a direct like-for-like comparison with published ΛCDM analyses [4, 5]. We analyze the Pantheon+ compilation of 1701 Type Ia supernovae together with a low-z calibrator subset ($z \leq 0.10$) anchored by Cepheid variable stars.

Simulations and fits for the Pantheon+ analysis were performed using two independent publicly available Python codes, `UMH_RedShiftPlus.py` and `UMH_vs_PantheonPlus.py`, ensuring no shared implementation artifacts. The independent DES-SN5YR/Dovekie validation was performed in a separate validation pipeline, `UMH_vs_DES_SN5YR.py`, using the DES-Dovekie ordered Hubble-diagram data vector and supplied STAT+SYS inverse covariance matrix.

2.2 UMH Redshift Law

In UMH, the observed redshift arises from the ratio of local clock rates at emission and reception. For a wave propagating through the medium, the general redshift law (derived in [1], Eqs. R1–R2) is:

$$1 + z \;=\; \exp\!\left(\int_\gamma \alpha(\mathbf{x}, \mathbf{k})\, ds\right) \cdot \frac{(u_e \cdot k)_e}{(u_o \cdot k)_o}, \tag{1}$$

where $\alpha(\mathbf{x}, \mathbf{k}) \equiv -\frac{d}{ds} \ln \chi(T, \rho)$ is a total derivative of the local clock-rate factor $\chi \equiv \sqrt{(T/\rho)/(T_u/\rho_u)}$. For a sufficiently homogeneous cosmological background, $\alpha(\mathbf{x}, \mathbf{k}) \approx \alpha = \text{const}$, and for comoving source and observer the kinematic factor is unity, giving:

$$1 + z \;=\; e^{\alpha d}, \qquad \text{i.e.} \quad z(d) \;=\; e^{\alpha d} - 1. \tag{2}$$

At low redshift this reduces to $z \approx \alpha d \approx (H_0/c)\, d$, identifying $\alpha = H_0/c$ as an attenuation coefficient analogous to an inverse Hubble length [2, 3]. Time dilation appears naturally as $(1 + z)$ due to the Lorentz-invariant strain propagation [1].

This is the UMH redshift–distance relation tested here.

The UMH distance-modulus model used for fitting is constructed multiplicatively from the UMH distance, time-dilation, and transmission terms as:

$$\mu = 5 \log_{10}\!\left[d(z)\,(1+z)^{(1+\delta)/2}\, T(z)^{-1/2}\right] + M_0, \tag{3}$$

$$d(z) = \frac{\ln(1+z)}{\alpha}, \tag{4}$$

$$T(z) = \exp\!\left[-\beta_1 \ln(1+z) - \beta_2 \ln^2(1+z)\right]. \tag{5}$$

Here M_0 is the profiled magnitude/intercept offset, absorbing the overall distance-scale normalization and fixed zero point, while β_1 and β_2 are empirical strain-transmission corrections unrelated to the SALT2 color term. The parameter δ governs the time-dilation scaling and is fixed at unity for Lorentz invariance.
In general UMH applications, (M_0, β_1, β_2) may be treated as nuisance parameters; however, in the specific Pantheon+ cosmological comparison below, α, β_1, β_2, and δ are determined once and then held fixed, and only M_0 is profiled.

In UMH these terms arise from the mechanical partition of oscillatory energy into longitudinal and transverse components as waves propagate through the UMH Formulation. Unlike interaction-based attenuation models (e.g. scattering or photon loss)[18], the β terms encode reversible strain-energy curvature and therefore do not break Etherington duality.

For small α, and with $\beta_1 = \beta_2 = 0$, $\delta = 1$, the UMH luminosity law approaches the standard low-redshift distance–redshift behavior recovered by ΛCDM, illustrating that UMH reproduces the observed SN Ia distance–redshift relation without invoking metric expansion.

Energy Conservation and Duality. The UMH luminosity formulation preserves energy conservation in the mechanical sense: wave energy flux decays as $1/r^2$ due to geometric spreading, while the apparent luminosity attenuation $(1+z)^2$ arises from cumulative redshift and time-dilation factors. Thus the standard Etherington distance-duality relation $D_L = (1+z)^2 D_A$ remains satisfied in form[6, 7], though its physical origin is strain-mediated energy transfer rather than metric expansion.
In the notation of Eq. 3, the effective luminosity distance may be written

$$D_L(z) = d(z)\,(1+z)^{(1+\delta)/2}\, T(z)^{-1/2}.$$

For the Lorentz-invariant value $\delta = 1$, this becomes

$$D_L(z) = d(z)\,(1+z)\,T(z)^{-1/2}.$$

The corresponding angular-diameter distance is defined with the same reversible strain-transfer factor,

$$D_A(z) = d(z)\,(1+z)^{-1}\,T(z)^{-1/2}.$$

Therefore

$$\frac{D_L}{D_A} = (1+z)^2,$$

so the broadband transmission term does not introduce luminosity-only opacity. The factor $T(z)$ rescales the inferred propagation geometry symmetrically in the luminosity and angular-diameter measures and therefore cancels from the duality ratio.

Transmission term. The broadband transmission term (Eq. 5) represents strain-mediated energy transfer within the UMH Formulation. These coefficients β_1 and β_2 are unrelated to the SALT2 color–luminosity parameter of the same symbol.

2.2.1 Parameter Classification and Degrees of Freedom

The UMH formulation contains three distinct classes of quantities:

1. A single *cosmological* scale parameter α;
2. *Non-cosmological* transfer coefficients (β_1, β_2);
3. The absolute-magnitude normalization M_0, profiled in direct analogy to standard SN Ia analyses.

Cosmological parameter α. UMH predicts that the accumulated strain in the medium produces the low-redshift relation:

$$L \equiv \ln(1+z) \simeq \alpha d \qquad (z \lesssim 0.1), \tag{6}$$

making α the sole cosmology-level degree of freedom in the redshift law. This scale is determined once from the $z \leq 0.10$ calibration sample and is held fixed for all subsequent Hubble-diagram fits, exactly paralleling the empirical determination of H_0 in standard ΛCDM analyses. In all Pantheon+ fits, α is fixed at the value obtained from the low-z calibration and is not refit.

Transfer coefficients (β_1, β_2). The broadband transmission term (Eq. 5) represents strain-mediated energy transfer within the UMH formulation. The coefficients β_1 and β_2 enter only through this transfer function. They modify the redshift-dependent broadband transmission shape but not the underlying UMH source–observer propagation law $d(z) = \ln(1+z)/\alpha$; once fixed, they define a fixed transmission function rather than additional degrees of freedom in the final Hubble-diagram likelihood. Accordingly, they are treated as fixed nuisance parameters and are not counted as additional cosmological degrees of freedom in model comparison. These coefficients are unrelated to the SALT2 color–luminosity parameter of the same symbol, but are analogous in role, though not in form, to nuisance parameters such as the color–luminosity and population-drift terms used in SALT2/BBC (BEAMS with Bias Corrections) supernova pipelines [10, 11].

With α fixed from the low-z calibration, β_1 and β_2 are inferred once from the Pantheon+ SN-only sample via generalized least squares (GLS) using the full STAT+SYS covariance and then held fixed, yielding $\beta_1 = 0.432 \pm 0.06$, $\beta_2 = -0.27 \pm 0.09$. This single-pass calibration is directly analogous to the determination of SALT2 nuisance parameters from the same SN Ia dataset: both enter the luminosity relation while leaving the underlying distance–redshift scaling unchanged. Sensitivity tests show that modest perturbations of β_1 and β_2 about their calibrated values shift the best-fit residuals only at subdominant levels relative to the intrinsic scatter of the Pantheon+ sample, leaving the preferred $\delta = 1$ time-dilation solution and the overall goodness of fit unchanged.

It is important to distinguish redshift dependence from likelihood freedom. The coefficients β_1 and β_2 multiply redshift-dependent basis functions in the broadband transmission law, and therefore affect the shape of the predicted Hubble diagram. However, a redshift-dependent correction does not constitute a free parameter in a given likelihood evaluation unless its coefficient is varied in that likelihood. In the final Pantheon+ and DES-SN5YR Hubble-diagram comparisons reported here, β_1 and β_2 are fixed transmission-law coefficients: they are not minimized, profiled, or scanned against the target Hubble diagram. The only parameter varied in the final UMH likelihood is the intercept M_0. Thus the conditional final-fit parameter count is $k = 1$ for UMH, corresponding to the single profiled nuisance intercept, even though the fixed transmission function itself is redshift dependent.

By contrast, removing the transmission term entirely, $\beta_1 = \beta_2 = 0$, introduces a smooth redshift-dependent residual rather than a uniform shift. When δ is allowed to vary, this biases the apparent best-fit time-dilation exponent to $\delta \approx 1.3$ and raises χ^2/dof slightly, from 0.898 to 0.902 (Figures 8 and 9). This effect reflects the removal of a broadband transmission correction, not a change in the UMH distance–redshift law. The cosmological scaling remains set by α alone; only the transmission structure, and through its partial degeneracy with the time-dilation term the apparent best-fit δ, changes.

Degrees of freedom for model comparison. Information criteria are reported under an explicitly conditional final-fit convention. In this convention, k counts only parameters varied in the final Pantheon+ Hubble-diagram likelihood. The absolute-magnitude/intercept parameter M_0 is analytically profiled in both models and is included in both absolute AIC/BIC values. The UMH final fit has $k = 1$, corresponding to M_0, because α is fixed by the independent low-redshift calibration and β_1, β_2, and δ are held fixed prior to the final Hubble-diagram comparison. The flat ΛCDM reference fit has $k = 2$, corresponding to M_0 and the fitted matter-density parameter Ω_m.

Thus the reported ΔAIC and ΔBIC values should be interpreted as conditional final-fit information criteria, not as penalties for the entire historical development or theoretical prior structure of either model. Under this convention, the difference $\Delta k = k_{\Lambda\mathrm{CDM}} - k_{\mathrm{UMH}} = 1$ reflects the fact that Ω_m is varied in the final flat-ΛCDM SN fit, whereas the UMH propagation scale α is fixed from the disjoint low-z calibration sample and not refit.

Although β_1 and β_2 are determined once in the UMH calibration pipeline, they are not refit in the Pantheon+ Hubble comparison and are therefore not included as free final-likelihood parameters. If one instead counts calibration-stage quantities appearing in the luminosity relation, the underlying χ^2 values are unchanged and the model comparison becomes a parameter-bookkeeping sensitivity test rather than a pure final-likelihood comparison. We therefore report both the conditional convention and a conservative sensitivity convention below.

Only α governs the UMH source–observer propagation law, as summarized in Table 1, and therefore constitutes the sole UMH cosmological redshift-scale parameter in the present analysis. The remaining quantities either describe fixed transmission corrections (β_1, β_2), a theoretically fixed time-dilation relation $(\delta = 1)$, or the standard absolute-magnitude normalization M_0, which is treated as a nuisance parameter in Type Ia supernova analyses. As in standard SN Ia cosmology, the low-z calibration fixes the overall distance scale but does not predetermine the functional form of the distance–redshift relation tested at higher redshift.

Table 1: Parameter classification used in the Pantheon+ analysis.

Parameter	Physical Role	Origin	Treatment in Pantheon+ Fit
α	Source–observer propagation parameter governing the UMH redshift–distance relation	Calibrated from the low-z SN Ia sample	Cosmological parameter
β_1	First-order transmission coefficient	Calibrated from the Pantheon+ SN-only sample (GLS, $\delta = 1$ fixed)	Held fixed (not refit)
β_2	Second-order transmission coefficient	Calibrated from the Pantheon+ SN-only sample (GLS, $\delta = 1$ fixed)	Held fixed (not refit)
δ	Time-dilation exponent	Lorentz-invariant UMH prediction ($\delta = 1$)	Theoretically fixed
M_0	Absolute magnitude normalization	Standard SN Ia nuisance parameter	Profiled nuisance parameter

Summarizes the parameter treatment used throughout this work. Only α governs the UMH source–observer propagation law. The coefficients β_1 and β_2 are calibrated once from the Pantheon+ SN-only sample and held fixed during the Hubble-diagram comparison. The time-dilation exponent is fixed to the Lorentz-invariant value $\delta = 1$, while M_0 is treated as the standard SN Ia nuisance parameter.

For completeness, alternative parameter-classification conventions can be applied when evaluating information criteria. In the present work, β_1 and β_2 are treated as fixed transmission-calibration coefficients, analogous to calibration and nuisance corrections commonly employed in standard SN Ia analyses. The primary AIC/BIC values use the conditional Pantheon+ Hubble-diagram likelihood, in which only parameters varied in the final distance–redshift fit are counted.

A more conservative sensitivity convention is also shown in Table 2. In this convention, fixed UMH calibration-stage quantities appearing in the luminosity relation are counted as model-side inputs even though they are not varied in the final Hubble-diagram likelihood. This convention changes the information-criterion penalty but not the underlying goodness-of-fit.

It is therefore best interpreted as a bookkeeping sensitivity test, not as the primary final-likelihood comparison.

Table 2: Parameter-count sensitivity for the Pantheon+ comparison.

Model	Counting convention	k	χ^2	AIC	BIC	Interpretation
UMH	Conditional final Pantheon+ fit	1	1456.8	1458.8	1464.2	Primary final-likelihood convention
ΛCDM	Conditional flat-SN fit	2	1457.0	1461.0	1471.8	Same final-likelihood convention
UMH	Conservative UMH-side bookkeeping	3	1456.8	1462.8	1479.0	Counts M_0, β_1, β_2
UMH	Full UMH luminosity-input bookkeeping	5	1456.8	1466.8	1493.8	Counts $M_0, \alpha, \beta_1, \beta_2, \delta$

Note. The first two rows give the conditional final-fit AIC/BIC comparison used in this paper. The lower rows show conservative UMH-side sensitivity conventions in which fixed calibration-stage quantities are counted even though they are not varied in the final Pantheon+ likelihood. These rows are not the primary model-selection convention; they show how the information-criterion penalty changes under stricter bookkeeping. In all rows the χ^2 value is unchanged because the fitted residuals and covariance treatment are unchanged.

2.3 Relation to Prior Non-Expansion Redshift Models

In the UMH framework[1], the redshift mechanism can be summarized as follows: a propagating strain field in a Lorentz-invariant medium undergoes cumulative phase evolution and reversible energy redistribution, such that the ratio of emission and reception clock rates is determined by the integrated strain history along the path, yielding an exponential redshift-distance relation.

UMH is not a tired-light or scattering-based non-expansion model. Historical non-expanding proposals (e.g., Zwicky attenuation, plasma scattering, conformal non-metric models) fail observational tests such as Tolman surface-brightness dimming and spectral-aging constraints[16, 17]. UMH differs fundamentally: its redshift arises from the endpoint clock-ratio in a Lorentz-invariant mechanical medium, not from photon loss, scattering, or dissipative transfer. As detailed in the full UMH framework[1], UMH preserves Etherington duality and predicts the observed $(1+z)$ time-dilation relation from first principles. Because these broader theoretical issues are addressed elsewhere, the present paper restricts attention to the narrow and well-posed test of the SN Ia Hubble diagram; an extensive comparison with historical non-expansion models is therefore unnecessary within this scope.

2.4 Statistical Methodology

We use the Pantheon+SH0ES supernova table (1701 SNe). The Hubble-diagram sample is the SN-only subset obtained by excluding the 77 Cepheid-calibrator rows (`IS_CALIBRATOR` $= 1$), leaving $N = 1624$ supernovae ($1701 - 77 = 1624$); the Pantheon+ outlier/quality and fit-availability flags supplied in the release are retained and remove no additional objects beyond the calibrator split. For each supernova the data vector is the corrected apparent magnitude $m_{b,\mathrm{corr}}$ at the flow-corrected redshift z_{HD}. The propagation scale α is determined separately from the Cepheid-calibrator subset (`IS_CALIBRATOR` $= 1$, $N = 77$; Section 3.1) and held fixed throughout, so the calibration and Hubble-diagram fits use disjoint subsets and no calibrator object is reused.

The full Pantheon+ STAT+SYS covariance matrix $\mathbf{C}$ [4, 5] is loaded from the published file, subselected to the same SN-only indices as the data vector, symmetrized as $\mathbf{C} \to \frac{1}{2}(\mathbf{C}+\mathbf{C}^T)$, and augmented with a numerical jitter term $10^{-12}\mathbf{I}$ for Cholesky stability only. The peculiar-velocity floor and intrinsic scatter are taken as encoded in $\mathbf{C}$.

Goodness of fit is computed by Cholesky solve as

$$\chi^2 = \Delta\mu^T\, \mathbf{C}^{-1}\, \Delta\mu, \qquad \Delta\mu = m_{b,\mathrm{corr}} - \mu_{\mathrm{model}}(z) - M_0,$$

where the absolute-magnitude/intercept offset M_0 is the only profiled nuisance parameter, determined analytically from the same covariance matrix,

$$M_0 = \frac{\mathbf{1}^T\mathbf{C}^{-1}\,(m_{b,\mathrm{corr}} - \mu_{\mathrm{model}})}{\mathbf{1}^T\mathbf{C}^{-1}\mathbf{1}}.$$

The UMH and ΛCDM fits are thus compared using the same data vector, covariance matrix, residual definition, and analytic profiling of M_0. For UMH, α is fixed from the low-z calibration and β_1, β_2, $\delta = 1$ are held fixed; the flat ΛCDM reference is fit by minimizing χ^2 over Ω_m, with M_0 profiled in the same way.

For model comparison we evaluate the conditional Akaike and Bayesian information criteria [12, 13],

$$\mathrm{AIC} = \chi^2 + 2k, \qquad \mathrm{BIC} = \chi^2 + k\ln N,$$

where k is the number of free parameters varied in the conditional Hubble-diagram fit and N is the number of supernovae. UMH ($\delta = 1$) and flat ΛCDM (Ω_m free) produce nearly identical residuals; under the conditional final-fit convention adopted here the information criteria are lower for UMH, with $\Delta\mathrm{AIC} = -2.2$ and $\Delta\mathrm{BIC} = -7.6$. Conservative parameter-counting alternatives are reported separately as bookkeeping sensitivities rather than as the primary final-likelihood comparison.

All fits were carried out independently in both codebases, which operate on the same data but implement the full pipeline separately and yield statistically indistinguishable results. Our ΛCDM baseline reproduces the official Pantheon+ χ^2 and information-criteria values to within rounding, confirming correct handling of the STAT+SYS covariance matrix.

Table 3: Statistical inputs and fit treatment used in the Pantheon+ comparison.

Quantity	**Treatment**
Dataset	Pantheon+SH0ES supernova table.
Hubble-diagram sample	SN-only subset with Cepheid calibrators excluded (IS_CALIBRATOR = 0), yielding $N = 1624$ supernovae.
Redshift variable	Pantheon+ flow-corrected redshift z_{HD}.
Data vector	Corrected apparent magnitude $m_{b,\mathrm{corr}}$.
Covariance	Full Pantheon+ STAT+SYS covariance, subselected to the same SN-only rows, symmetrized, and used in all χ^2 evaluations.
Residual definition	$\Delta\mu = m_{b,\mathrm{corr}} - \mu_{\mathrm{model}}(z) - M_0$.
Profiled parameter	M_0, analytically profiled using C^{-1}.
UMH fixed quantities	α from low-z calibration; β_1, β_2 fixed after calibration; $\delta = 1$.
ΛCDM fit	Flat ΛCDM with Ω_m minimized over and M_0 analytically profiled.
Model comparison	AIC $= \chi^2 + 2k$ and BIC $= \chi^2 + k\ln N$.

3 Results

3.1 Low-z Calibration

A regression of comoving distance against $L = \ln(1+z)$ for 77 calibrators yields $\alpha = (2.48 \pm 0.08) \times 10^{-4}\,\mathrm{Mpc}^{-1}$, equivalent to $H_0 = 74.4 \pm 2.3\,\mathrm{km\,s^{-1}\,Mpc^{-1}}$. Figure 1 shows the approximately linear relationship between $\ln(1+z)$ and comoving distance in the low-z regime, with the fitted slope corresponding to the calibrated value of α. The fit quality ($\chi^2/\mathrm{dof} = 0.34$) indicates no excess scatter beyond observational uncertainties; the sub-unity value reflects conservative (and partly correlated) calibrator uncertainties rather than overfitting, and does not bias the central value of α. This is consistent with local Hubble determinations without introducing expansion[3].

This calibration procedure mirrors the SH0ES (Supernovae and H_0 for the Equation of State) determination, in which a low-redshift subset is used to fix the distance scale, while the higher-redshift sample provides an independent test of the distance–redshift relation. In this analysis, the propagation scale α is fixed by the low-redshift calibration and is not refit to the full dataset.

The low-z calibration fits

$$d = c_0 + c_1\,\ln(1+z), \qquad \alpha = 1/c_1, \tag{7}$$

using robust Huber iteratively reweighted least-squares (IRLS) weighting to reduce leverage from outliers[14].

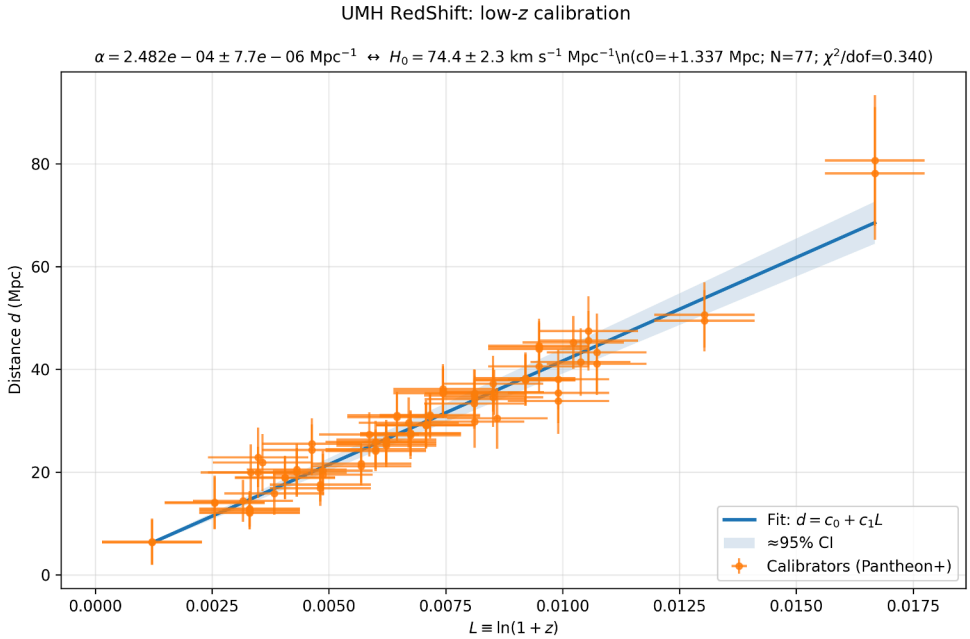

Figure 1: Redshift pipeline: Low-z calibration of the UMH redshift relation.
The best-fit $\alpha = (2.48 \pm 0.08) \times 10^{-4}\,\mathrm{Mpc}^{-1}$ corresponds to $H_0 = 74.4 \pm 2.3\,\mathrm{km\,s^{-1}\,Mpc^{-1}}$.

Table 4: High-redshift validation after excluding progressively larger low-redshift regions.

Redshift Cut	**N**	$\boldsymbol{\chi^2}$	**dof**	$\boldsymbol{\chi^2/\mathrm{dof}}$
$z > 0.10$	960	834.65	959	0.8703
$z > 0.15$	875	775.71	874	0.8875
$z > 0.20$	753	618.60	752	0.8226

As a high-redshift validation test, the calibrated UMH parameters α, β_1, β_2, and $\delta = 1$ were held fixed while only the nuisance intercept M_0 was re-profiled after excluding progressively larger low-redshift regions. The resulting fits for $z > 0.10$, $z > 0.15$, and $z > 0.20$ remain statistically stable, indicating that the Pantheon+ agreement is not driven by reuse of the low-redshift calibration region.

3.2 Pantheon+ Hubble Fit

Applying the UMH redshift law to the full Pantheon+ dataset reproduces the Hubble diagram with statistically comparable fit to ΛCDM (Figure 2).

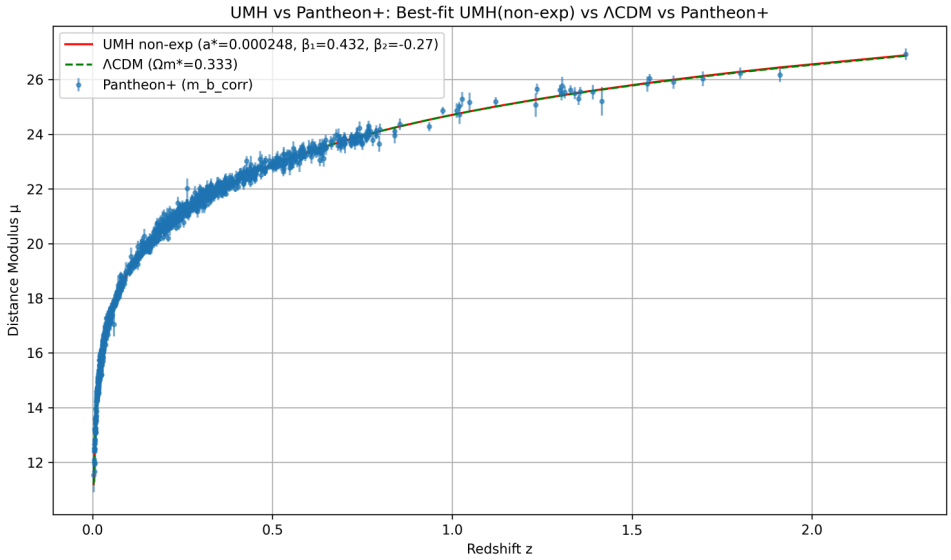

Figure 2: Pantheon+ pipeline: comparison of UMH (solid red) and ΛCDM (green dashed) models. Both reproduce the observed distance–modulus–redshift relation across $0 < z < 2.3$. In the figure legends, a^* denotes the calibrated α and Ω_m^* the best-fit matter density.

Although the UMH and flat ΛCDM formulations produce closely degenerate Hubble-diagram observables over the Pantheon+ redshift range, their underlying luminosity-distance relations are not identical. The flat ΛCDM reference fit gives $\Omega_m = 0.333 \pm 0.018$, with M_0 analytically profiled. The nuisance intercept M_0 is analytically profiled in both models and is not assigned independent physical interpretation because it absorbs the SN Ia absolute-magnitude zero point. Figure 3 shows the fractional difference

$$\frac{d_{L,\mathrm{UMH}} - d_{L,\Lambda\mathrm{CDM}}}{d_{L,\Lambda\mathrm{CDM}}}$$

computed using the UMH calibration and the reference flat ΛCDM model. The nonzero, redshift-dependent fractional difference demonstrates that the UMH luminosity-distance relation is not algebraically equivalent to the ΛCDM distance law, despite producing a statistically comparable fit to the Pantheon+ observations.

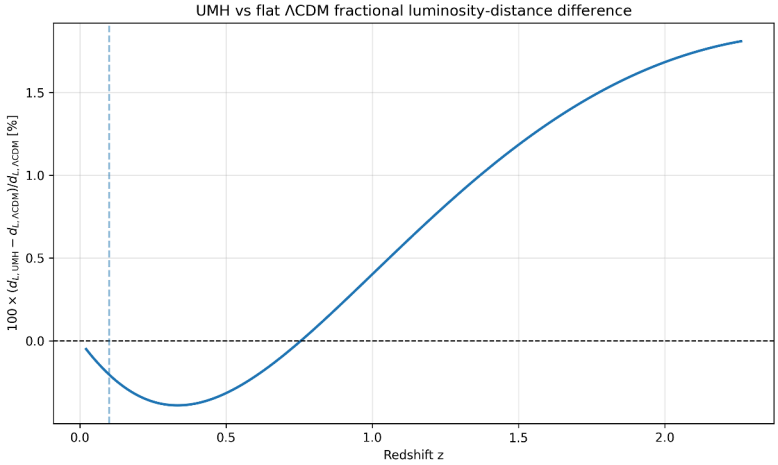

Figure 3: Redshift pipeline: Fractional luminosity-distance difference between the UMH formulation and flat ΛCDM ($\Omega_m = 0.333$, $H_0 = 74.4\,\mathrm{km\,s^{-1}\,Mpc^{-1}}$), with both models evaluated at the UMH-calibrated H_0 to isolate the functional-form difference. The fractional difference ranges from -0.4% near $z \approx 0.3$ to $+1.8\%$ at $z \approx 2.3$, with a sign change near $z \approx 0.75$, demonstrating that the two distance–redshift relations are not algebraically identical. The sub-percent to low-percent shape difference explains why both models produce statistically comparable fits to the Pantheon+ SN Ia data despite being functionally distinct. The vertical dashed line marks the low-z calibration boundary ($z = 0.10$).

Residuals show no systematic drift (slope $m = 0.016 \pm 0.023$), with whitened residuals consistent with $N(0, 1)$ (Figure 4). These results indicate no evidence of systematic bias in the fit.

Results remain stable (parameter shifts $< 1\sigma$) under jackknife resampling and varying outlier-mask definitions, confirming that the UMH fit is robust to sample composition and data-selection effects.

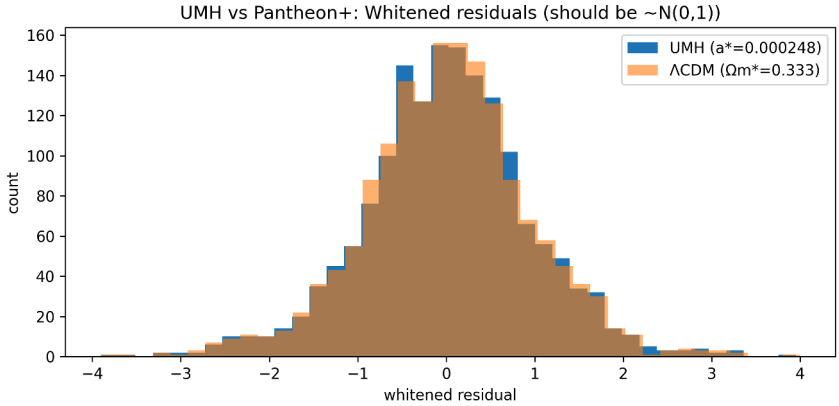

Figure 4: Pantheon+ pipeline: Whitened residuals of the Pantheon+ fit. The residual distributions for both UMH and ΛCDM are consistent with Gaussian noise and show no visible systematic structure.

3.3 Independent DES-SN5YR Validation

As an independent cross-dataset validation, the same UMH final-fit procedure was applied to the DES-SN5YR/Dovekie Hubble diagram. The DES analysis used the ordered DES-Dovekie distance-modulus vector with $N = 1820$ supernovae and the supplied STAT+SYS inverse covariance matrix. The DES residuals were defined using the same form as in the Pantheon+ analysis, $\Delta\mu = \mu_{\rm data} - \mu_{\rm model} - M_0$, and the intercept M_0 was analytically profiled using the supplied STAT+SYS inverse covariance matrix before evaluating χ^2. The UMH propagation scale was fixed to the Pantheon+/Cepheid value,

$$\alpha = 2.481805 \times 10^{-4}\,\mathrm{Mpc}^{-1},$$

and the transmission coefficients were recovered using the same generalized least-squares transmission fit. The DES-SN5YR/ Dovekie data release and associated covariance inputs are publicly available from the DES-SN5YR repository, and the Dovekie recalibration is described in the DES reanalysis literature[21, 22].

The DES-SN5YR sample independently recovers transmission coefficients consistent with the Pantheon+ values:

$$\beta_1 = 0.435, \qquad \beta_2 = -0.275,$$

compared with the Pantheon+ recovery $\beta_1 \simeq 0.432$ and $\beta_2 \simeq -0.270$. With these coefficients fixed and only M_0 profiled, UMH gives $\chi^2 = 1631.7$ for $N = 1820$, statistically indistinguishable from the flat ΛCDM fit, $\chi^2 = 1631.8$ with $\Omega_m = 0.329$. The UMH residual slope is consistent with zero, $m = 0.016 \pm 0.020$ mag per unit redshift.

The purpose of the DES-SN5YR recovery is therefore not to introduce a new DES-specific pair of free parameters, but to test whether the same transmission coefficients are recovered when the UMH transmission law is applied to a substantially independent SN Ia Hubble diagram. Once recovered, the coefficients are held fixed in the DES final-likelihood comparison in exactly the same way as in the Pantheon+ final-likelihood comparison. As fixed-coefficient transfer checks, the DES-SN5YR recovered values were inserted directly into the Pantheon+ likelihood, and the Pantheon+ recovered values were inserted directly into the DES-SN5YR likelihood, without refitting or profiling either transmission coefficient. In both directions, the target-dataset χ^2, residual slope, AIC, and BIC are unchanged at the quoted precision, with only M_0 profiled. These bidirectional transfer tests show that the Pantheon+ and DES-SN5YR fits do not rely on dataset-specific adjustment of β_1 and β_2.

Table 5: Independent DES-SN5YR/Dovekie validation and fixed-coefficient transfer test of UMH transmission coefficients.

Target dataset / Model	**Source of β_1, β_2**	$\boldsymbol{\beta_1}$	$\boldsymbol{\beta_2}$	$\boldsymbol{\chi^2}$	**N**	**Residual slope**	$\boldsymbol{\Omega_m}$	**AIC**	**BIC**
Pantheon+ UMH	Pantheon+ recovery	0.432	−0.270	1456.8	1624	0.016 ± 0.023	—	1458.8	1464.2
Pantheon+ UMH	DES-SN5YR recovery	0.435	−0.275	1456.8	1624	0.016 ± 0.023	—	1458.8	1464.2
DES-SN5YR UMH	DES-SN5YR recovery	0.435	−0.275	1631.7	1820	0.016 ± 0.020	—	1633.7	1639.2
DES-SN5YR UMH	Pantheon+ recovery	0.432	−0.270	1631.7	1820	0.016 ± 0.020	—	1633.7	1639.2
DES-SN5YR ΛCDM	—	—	—	1631.8	1820	0.001 ± 0.020	0.329	1635.8	1646.8

Note. In all UMH rows, α and the transmission coefficients are fixed before the target Hubble-diagram likelihood is evaluated; only M_0 is profiled. The transfer rows insert coefficients recovered from one SN Ia compilation directly into the other compilation without refitting either coefficient. The unchanged χ^2, residual slopes, AIC, and BIC show that the UMH agreement is not dependent on Pantheon+-specific or DES-specific adjustment of β_1, β_2.

The DES-SN5YR result is therefore a direct robustness test of the parameter-counting convention used above. It shows that the transmission coefficients inferred from Pantheon+ are not unique to that compilation: a substantially independent SN Ia Hubble diagram recovers the same coefficients and reproduces the same near-degeneracy with flat ΛCDM in χ^2, residual slope, and conditional AIC/BIC behavior.

3.4 Time Dilation and Robustness

The UMH fit with $\delta = 1$ includes the standard SN Ia $(1+z)$ time-dilation scaling, corresponding to the usual $(1+z)^{1/2}$ contribution to the distance modulus (Figure 5). The present analysis examines the time-dilation behavior implied by the UMH propagation law and does not constitute a separate fit to supernova light-curve stretch measurements. Diagnostic sensitivity tests of the transmission coefficients demonstrate that setting $\beta_1 = \beta_2 = 0$ produces an artificial minimum near $\delta = 1.3$, while restoring the calibrated β_1, β_2 coefficients recovers $\delta = 1$. This recovery reflects a first-order degeneracy between the time-dilation exponent and the first-order transmission coefficient. To first order in $\ln(1+z)$, the distance modulus (Eq. 3) depends on δ and β_1 only through the combination $\gamma \equiv \delta + \beta_1$, since the term linear in $\ln(1+z)$ carries a coefficient proportional to $(1+\delta+\beta_1)$. The Pantheon+ fit constrains this combination to $\gamma \approx 1.45$ (consistent with the calibrated $\delta + \beta_1 = 1 + 0.432$). Restoring the calibrated $\beta_1 = 0.432$ then yields an implied time-dilation exponent $\delta = \gamma - \beta_1 \approx 1.0$, recovering the Lorentz-invariant value, whereas setting $\beta_1 = 0$ forces the equivalent exponent to $\delta = \gamma \approx 1.45$—the "$\delta$-equivalent from γ" curve shown in Figs. 5 and 10. This linear-order equivalent ($\delta \approx 1.45$) is distinct from the $\delta \approx 1.3$ minimum obtained from the full χ^2 scan with $\beta_1 = \beta_2 = 0$ (Figs. 8 and 9), which additionally removes the second-order transmission term and re-optimizes against the data. These robustness checks demonstrate that UMH's physical time dilation is consistent with special relativity[8].

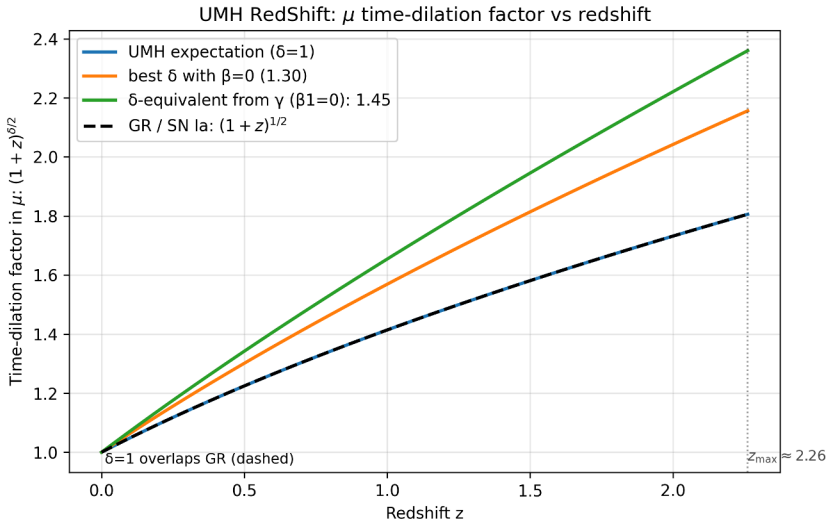

Figure 5: Redshift pipeline: Contribution of the model-implied time-dilation factor to the distance modulus, parameterized as $(1+z)^{\delta/2}$. The UMH prediction $\delta = 1$ overlaps the standard SN Ia/GR scaling. This diagnostic illustrates the time-dilation factor used in the Hubble-diagram relation and is not an independent fit to light-curve stretch measurements.

Within the UMH propagation model, the $(1+z)$ time-dilation factor follows analytically from the same redshift law used in the Hubble-diagram fit, corresponding to the standard $(1+z)^{1/2}$ contribution to the distance modulus. The value $\delta = 1$ is fixed by the underlying wave-medium mechanics and is not empirically tuned in the final Hubble-diagram likelihood.

4 Discussion

UMH is consistent with Pantheon+ results and low-z calibration, reproducing the observed redshift, distance modulus, and time-dilation relations within a non-expansion formulation. Beyond statistical model comparison, the key distinction between UMH and ΛCDM lies in the physical interpretation of the redshift mechanism. In ΛCDM, the distance–redshift relation arises from a metric expansion history governed by multiple energy components. In UMH, the same observables emerge from a propagation effect in a Lorentz-invariant medium with a single cosmological scaling parameter, without explicitly invoking a global expansion assumption within this framework.

The redshift-dependent fractional difference shown in Fig. 3 — evaluated at matched H_0 to isolate the functional form — ranges from approximately -0.4% near $z \approx 0.3$ to $+1.8\%$ at $z \approx 2.3$, with a sign change near $z \approx 0.75$. This demonstrates that the UMH luminosity-distance relation is not algebraically equivalent to the flat ΛCDM distance law. The close agreement over the Pantheon+ redshift range therefore reflects an observational degeneracy within the SN Ia domain rather than an explicit construction of the UMH relation to reproduce the ΛCDM distance law.

Within the UMH model, the standard SN Ia $(1 + z)$ time-dilation factor used in the Hubble-diagram relation arises from the same source–observer propagation law that governs the redshift and luminosity-distance relations. For the Lorentz-invariant value $\delta = 1$, the model yields

$$S(z) = 1 + z,$$

recovering the observed SN Ia time-stretch scaling as a direct consequence of the UMH propagation framework.

The use of independent codebases to implement the analysis reinforces the robustness of the result and mitigates implementation-specific artifacts. This demonstrates empirical consistency of the UMH formulation with the observed supernova data. Because Type Ia supernovae constrain only the observed distance–redshift and time-dilation relations [4, 5], they cannot by themselves distinguish metric expansion from distinct Lorentz-invariant redshift mechanisms that reproduce the same observables. Breaking this degeneracy requires independent observables that probe additional aspects of cosmology, including baryon acoustic oscillations (BAO), cosmic microwave background (CMB) anisotropies, gravitational-wave standard sirens, structure growth, weak lensing, Big Bang nucleosynthesis (BBN), and the full expansion history. These provide complementary constraints on expansion history, curvature, and propagation effects, and are therefore essential for distinguishing between competing physical interpretations of redshift. Such analyses are addressed in separate studies within the UMH framework.

The independent DES-SN5YR/Dovekie validation provides an additional check on the interpretation of the transmission coefficients. If β_1 and β_2 were merely Pantheon+-specific absorbers, one would not expect a separate SN Ia compilation with different calibration and covariance structure to recover nearly the same values. Instead, DES-SN5YR recovers $\beta_1 \simeq 0.435$ and $\beta_2 \simeq -0.275$, consistent with the Pantheon+ values $\beta_1 \simeq 0.432$ and $\beta_2 \simeq -0.270$. Moreover, bidirectional fixed-coefficient transfer tests show that DES-recovered coefficients reproduce the Pantheon+ likelihood, and Pantheon+-recovered coefficients reproduce the DES-SN5YR likelihood, with unchanged χ^2, residual slopes, AIC, and BIC at the quoted precision. This supports treating the coefficients as stable transmission-calibration inputs in the conditional final-fit comparison, while still leaving broader cosmological validation to independent probes outside the SN Ia Hubble diagram.

The fixed-coefficient transfer test strengthens this interpretation: inserting the DES-SN5YR recovered values directly into the Pantheon+ likelihood leaves the Pantheon+ χ^2, residual slope, AIC, and BIC unchanged at the quoted precision. Thus the Pantheon+ fit does not rely on Pantheon+-specific retuning of β_1 and β_2.

Within the standard ΛCDM interpretation, the SN Ia distance–redshift relation is modeled through a cosmological expansion history that includes a dark energy component. In contrast, the UMH formulation reproduces these observables through a different physical mechanism, without requiring an explicit dark energy term within this observational framework.

5 Robustness and Diagnostics

To show the results are not artifacts of a single pipeline, survey region, or nuisance-parameter choice, we provide diagnostics for both the Pantheon+ and Redshift analyses. The diagnostics shown in Figures 6 – 11 test the stability and internal consistency of the UMH fit under variations in nuisance-parameter treatment and data representation.

5.1 Redshift diagnostics

Figures 6 and 7 show that residuals remain centered near zero across redshift, both in raw and binned form, indicating no systematic deviation in the UMH fit. Figures 8 and 9 demonstrate that removing the calibrated transmission coefficients by setting $\beta_1 = \beta_2 = 0$ shifts the apparent minimum in the time-dilation exponent δ, while restoring the calibrated transmission coefficients recovers the physically expected $\delta = 1$ solution. Figures 10 and 11 show, respectively, the model-implied $(1+z)$ time-dilation scaling and the approximately Gaussian residual distribution with mild skewness and kurtosis.

Together, these diagnostics show that the UMH fit is stable, statistically well-behaved, and consistent with standard SN Ia observational constraints.

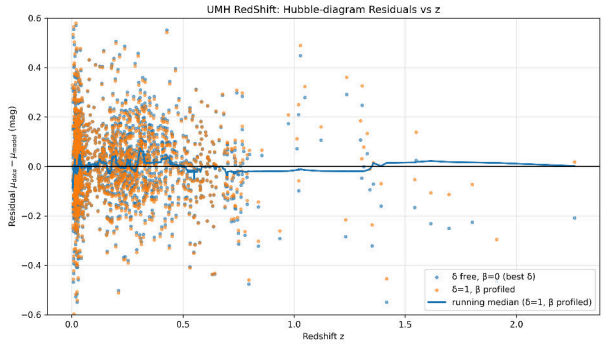

Figure 6: Redshift pipeline: Hubble-diagram residuals for the preferred UMH configuration ($\delta = 1$) with calibrated transmission coefficients, compared with the diagnostic case ($\beta_1 = \beta_2 = 0$, δ free). The running median of the preferred fit remains consistent with zero across redshift, indicating no systematic bias.

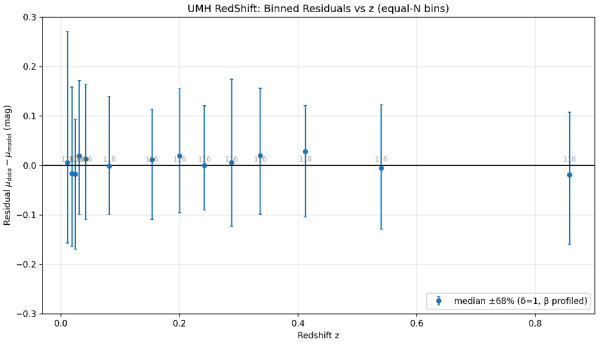

Figure 7: Redshift pipeline: Equal-count binned residuals versus redshift for the preferred UMH configuration ($\delta = 1$) with calibrated transmission coefficients. Bin medians are consistent with zero within 1σ uncertainties, with no evidence of systematic trends across redshift.

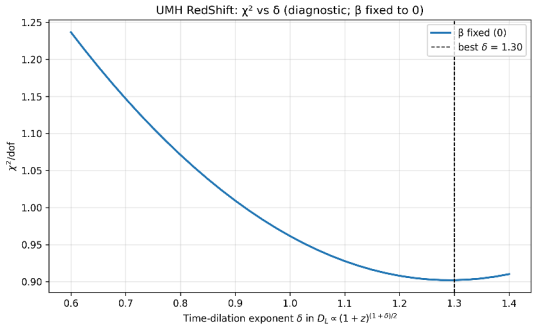

Figure 8: Redshift pipeline: chi-square per degree of freedom vs time-dilation exponent δ with $\beta_1 = \beta_2 = 0$ fixed to 0. A shallow minimum appears near $\delta \approx 1.3$, indicating that fixing $\beta_1 = \beta_2 = 0$ biases the preferred time-dilation exponent away from the physically expected $\delta = 1$.

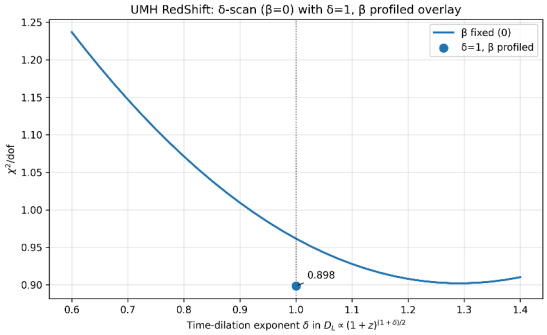

Figure 9: Overlay of the δ-scan for the diagnostic case $\beta_1 = \beta_2 = 0$ and the preferred calibrated-transmission point at $\delta = 1$. Restoring the calibrated transmission coefficients recovers the standard relativistic time-stretch value and improves the fit relative to the $\beta_1 = \beta_2 = 0$ diagnostic scan.

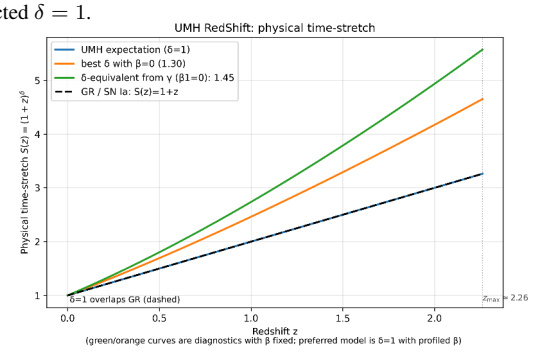

Figure 10: Model-implied physical time-stretch scaling $S(z) = (1+z)^{\delta}$. The UMH expectation $\delta = 1$ coincides with the standard SN Ia relation $S(z) = 1 + z$. This figure shows the propagation-law scaling used in the Hubble-diagram model, not a separate light-curve stretch fit.

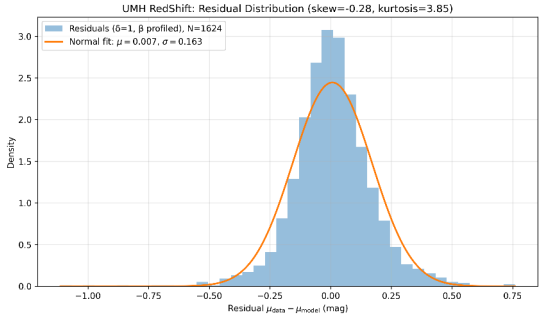

Figure 11: Redshift pipeline: Residual distribution for the preferred UMH configuration ($\delta = 1$) with calibrated transmission coefficients, shown with a Gaussian overlay. The distribution is approximately normal with mean $\mu = 0.007$ and standard deviation $\sigma = 0.163$, exhibiting mild skewness (-0.28) and slightly elevated kurtosis (3.85), consistent with typical SN Ia samples.

5.2 Pantheon+ diagnostics

Figures 12–16 provide complementary diagnostics of the Pantheon+ fit through multiple projections of the residual structure.

Residuals plotted against redshift and $\ln(1+z)$ (Figures 12 and 13) show no statistically significant slope, indicating the absence of long-range systematic drift. Equal-count binned residuals (Figure 14) remain consistent with zero within uncertainties across all redshift bins. Figure 15 shows the residual comparison between UMH and ΛCDM best fits, with highly similar structure, supporting statistically comparable fit quality. Figure 16 shows a zoomed view of the high-redshift ($z > 1.5$) residuals, where both UMH and ΛCDM remain consistent with statistical scatter and exhibit no systematic departures.

These diagnostics show that the UMH formulation reproduces the Pantheon+ observations without introducing systematic deviations relative to the standard cosmological model.

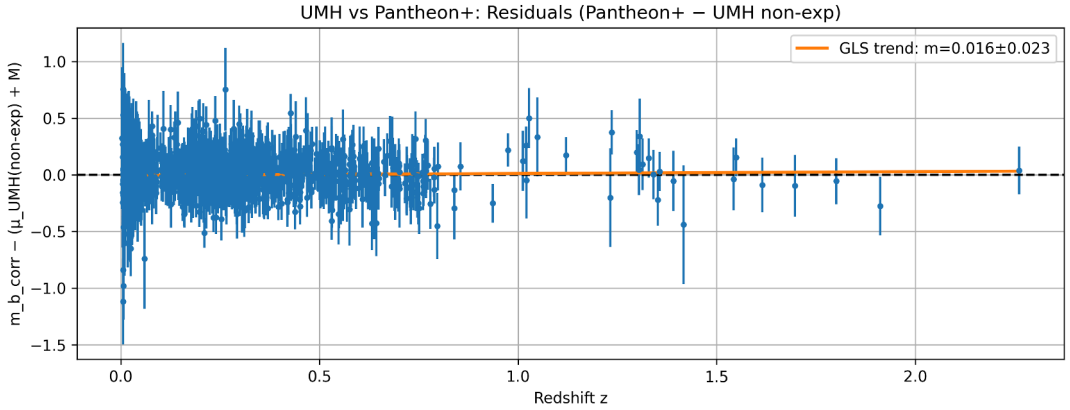

Figure 12: Pantheon+ pipeline: standardized distance-modulus residuals (data minus UMH model) versus redshift, with a generalized least-squares (GLS) trend. The fitted slope ($m = 0.016 \pm 0.023$) is consistent with zero, indicating no systematic redshift-dependent deviation.

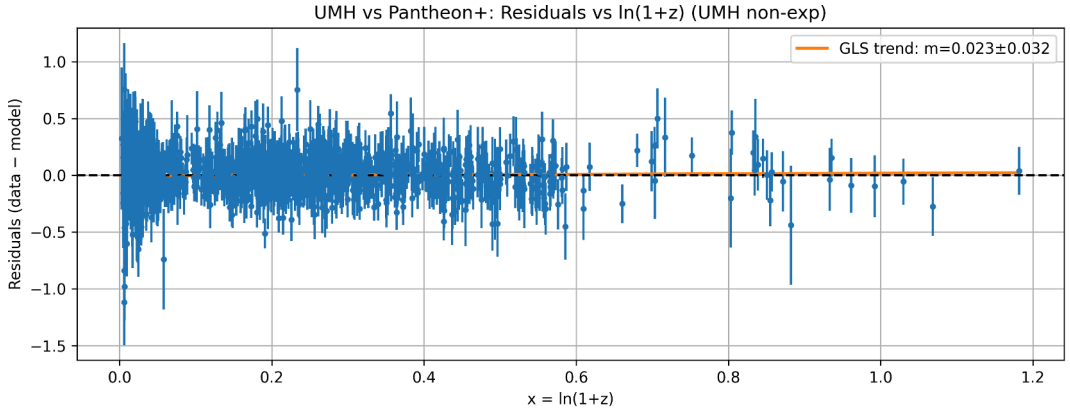

Figure 13: Pantheon+ pipeline: standardized distance-modulus residuals versus $L = \ln(1+z)$ (UMH natural variable), with a generalized least-squares (GLS) trend. The fitted slope ($m = 0.023 \pm 0.032$) is consistent with zero, indicating no long-range or systematic drift.

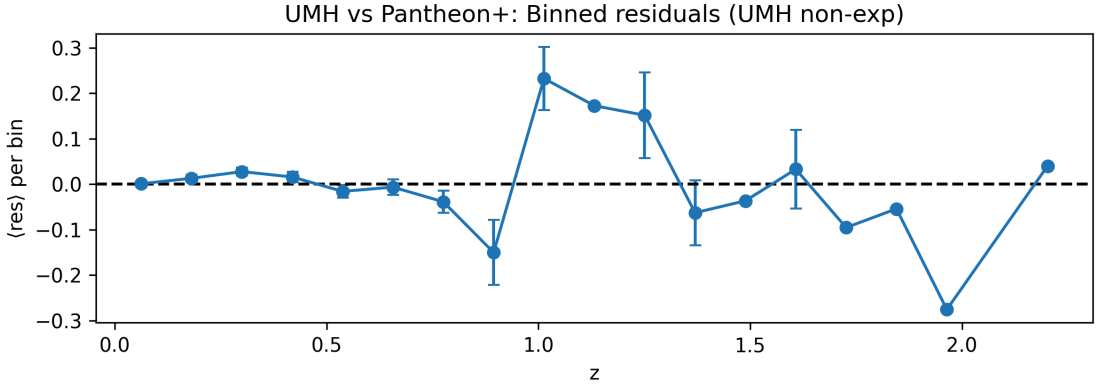

Figure 14: Pantheon+ pipeline: equal-count binned standardized distance-modulus residuals with $\pm 1\sigma$ uncertainties per bin. The binned residuals are consistent with zero within uncertainties, with no evidence of a statistically significant redshift-dependent trend.

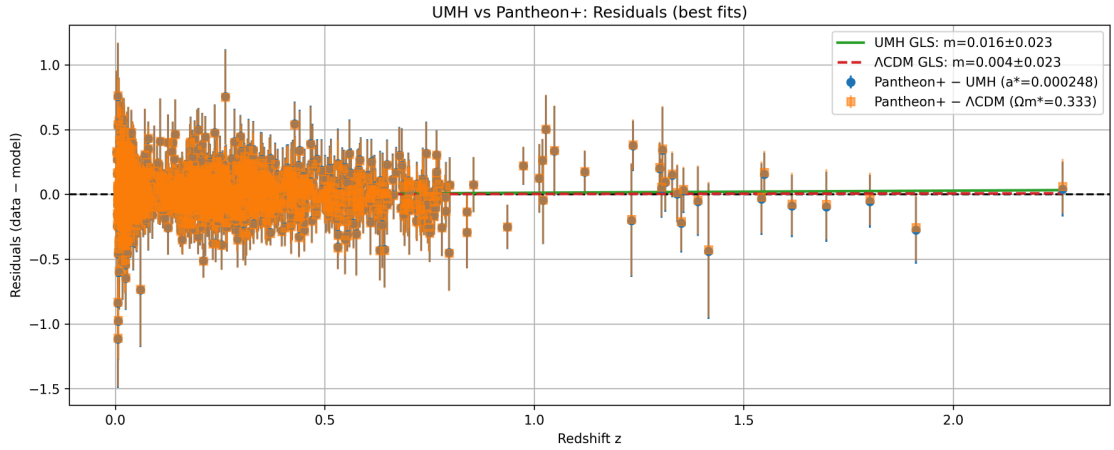

Figure 15: Pantheon+ pipeline: standardized distance-modulus residuals for UMH and ΛCDM best-fit models versus redshift, with generalized least-squares (GLS) trends. The residual distributions and trends are visually similar, with both models showing slopes consistent with zero, indicating no systematic redshift-dependent deviations.

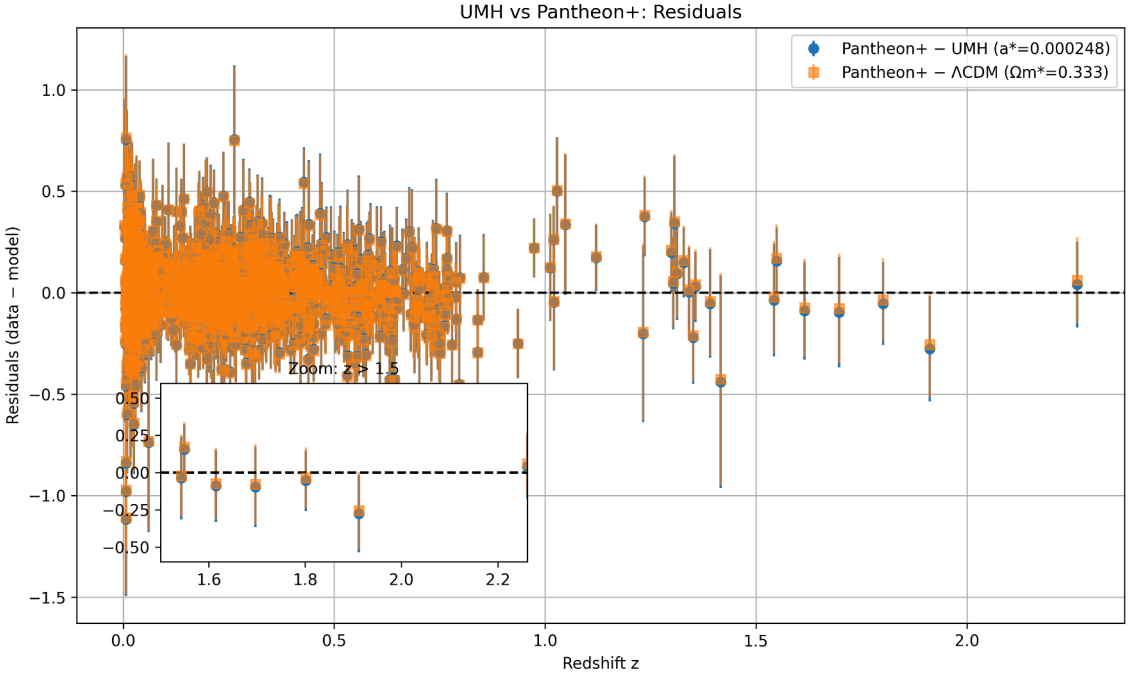

Figure 16: Pantheon+ pipeline: residual comparison for UMH and ΛCDM best-fit models, with inset showing a zoom on the high-redshift tail ($z > 1.5$). Residuals in this regime remain consistent with statistical scatter, with no evidence of systematic deviation despite larger uncertainties.

Figure 17 provides the analogous DES-SN5YR residual diagnostic. The UMH and flat ΛCDM residual trends are both consistent with zero, matching the Pantheon+ behavior and supporting the cross-dataset stability of the UMH Hubble-diagram fit.

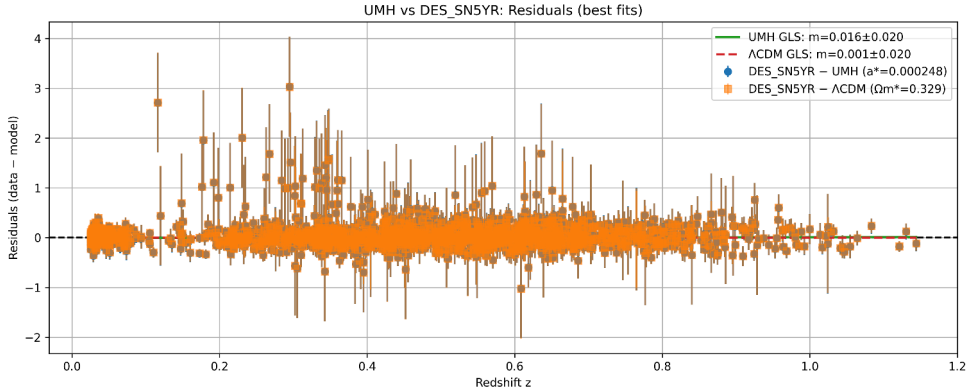

Figure 17: DES-SN5YR residual comparison for the best-fit UMH and flat ΛCDM models. Generalized least-squares trend fits give $m = 0.016 \pm 0.020$ for UMH and $m = 0.001 \pm 0.020$ for ΛCDM, both statistically consistent with zero. The independent DES dataset therefore reproduces the same residual behavior observed in Pantheon+, providing an external validation of the UMH distance-redshift formulation.

6 Conclusion

The UMH Formulation provides a self-consistent redshift and luminosity model that reproduces the SN Ia observables examined here:

- Pantheon+ SN Ia Hubble relation
- The associated $(1 + z)$ time-dilation scaling
- Consistent reproduction of redshift observables without requiring an explicit dark energy term within this observational framework

Table 6: **Pantheon+ Model Comparison Results**

Model	Fitted Parameters	k (effective)	χ^2	AIC	BIC	ΔAIC	ΔBIC
UMH	M_0 (free); α, β_1, β_2, δ (fixed)	**1**	**1456.8**	**1458.8**	**1464.2**	**-2.2**	**-7.6**
ΛCDM	M_0, Ω_m (free)	2	1457.0	1461.0	1471.8	0.0	0.0

Under the conditional Pantheon+ final-fit convention, k counts parameters varied in the Hubble-diagram likelihood. UMH has $k = 1$ because M_0 is profiled while α is fixed from the disjoint low-z calibration and β_1, β_2, δ are held fixed prior to the final fit. Flat ΛCDM has $k = 2$ because M_0 is profiled and Ω_m is varied. The reported AIC/BIC values are therefore conditional final-fit information criteria; conservative bookkeeping sensitivities are given in Table 2.

For this analysis, success is defined as reproducing the Pantheon+ distance-redshift relation, time-dilation behavior, and residual structure with statistically comparable fit quality to ΛCDM under the full STAT+SYS covariance. Conceptually, the low-redshift calibration fixes the overall distance scale ("the ruler length"), while the shape of the distance–redshift relation at higher redshift constitutes a forward prediction of the model.

The present SN Ia analysis does not by itself establish full cosmological viability, and does not yet test the broader set of independent observables required to distinguish complete cosmological models, including structure growth, weak lensing, Big Bang nucleosynthesis (BBN), and the full expansion history. Subsequent papers will present the corresponding Laser Interferometer Gravitational-Wave Observatory (LIGO) gravitational-wave chirps, Baryon Acoustic Oscillation (BAO), Cosmic Microwave Background (CMB), and related observable analyses using the same UMH framework [19, 20]. Additional theoretical context is available in [1].

This work provides a direct observational consistency test of the UMH redshift formulation against Pantheon+ SN Ia observations, with an independent DES-SN5YR/Dovekie validation showing that the fitted transmission coefficients are stable across SN Ia compilations.

Data and Code Availability

All simulation and analysis code used in this study, including `UMH_RedShiftPlus.py`, `UMH_vs_PantheonPlus.py`, `UMH_vs_DES_SN5YR.py`, and associated data processing scripts, are publicly available at the official UMH repository:
`https://github.com/UltronicPhysics/UMH`

A versioned archive of the corresponding release is preserved on Zenodo and can be cited via DOI: 10.5281/zenodo.16651832. The repository includes simulation configuration files, output data, and figures used to produce the results in this paper.

References

[1] Dodge, A. (2025). The Ultronic Medium Hypothesis (UMH): A Mechanical Foundation Wave-Based Model of Reality. Zenodo. https://doi.org/10.5281/zenodo.17497461
[2] Hubble, E. P. (1929). A Relation Between Distance and Radial Velocity Among Extra-Galactic Nebulae. *PNAS*, **15**(3), 168–173.
[3] Riess, A. G., Yuan, W., Macri, L. M., et al. (2022). A Comprehensive Measurement of the Local Value of the Hubble Constant. *ApJ*, **934**(1), 7.
[4] Scolnic, D., Brout, D., Carr, A., et al. (2022). The Pantheon+ Analysis: The Full Data Set. *ApJ*, **938**(2), 113.
[5] Brout, D., Scolnic, D., Popovic, B., et al. (2022). The Pantheon+ Analysis: Cosmological Constraints. *ApJ*, **938**(2), 110.
[6] Etherington, I. M. H. (1933). On the Definition of Distance in General Relativity. *Phil. Mag.*, **15**, 761–773.
[7] Ellis, G. F. R. (2007). Etherington's distance duality relation. *Gen. Relativ. Gravit.*, **39**, 1047–1052.
[8] Einstein, A. (1905). On the Electrodynamics of Moving Bodies. *Annalen der Physik*, **17**, 891–921.
[9] Lorentz, H. A. (1904). Electromagnetic phenomena in moving systems. *Proc. Royal Netherlands Acad.*, **6**, 809–831.
[10] Guy, J., Astier, P., Baumont, S., et al. (2007). SALT2 supernova model. *A&A*, **466**, 11–21.
[11] Betoule, M., Kessler, R., Guy, J., et al. (2014). JLA supernova analysis. *A&A*, **568**, A22.
[12] Akaike, H. (1974). Statistical model identification. *IEEE Trans. Auto. Control*, **19**, 716–723.
[13] Schwarz, G. (1978). Estimating model dimension. *Ann. Stat.*, **6**, 461–464.
[14] Huber, P. J. (1964). Robust estimation. *Ann. Math. Stat.*, **35**, 73–101.
[15] Goldhaber, G., Groom, D. E., Kim, A., et al. (2001). SN Ia time dilation. *ApJ*, **558**, 359–368.
[16] Tolman, R. C. (1930). Distance in expanding universe. *PNAS*, **16**, 511–520.
[17] Lubin, L. M., & Sandage, A. (2001). Tolman surface brightness test. *AJ*, **122**, 1084–1103.
[18] Zwicky, F. (1929). Redshift without expansion. *PNAS*, **15**, 773–779.
[19] Eisenstein, D. J., et al. (2005). BAO detection. *ApJ*, **633**, 560–574.
[20] Planck Collaboration (2018). Cosmological parameters. *A&A*, **641**, A6.
[21] Popovic, B., et al. (2025). The Dark Energy Survey Supernova Program: A Reanalysis of Cosmology Results and Evidence for Evolving Dark Energy with an Updated Type Ia Supernova Calibration. *arXiv:2511.07517*.
[22] Dark Energy Survey Collaboration. (2025). DES-SN5YR / DES-Dovekie cosmology data release. https://github.com/des-science/DES-SN5YR.